*International Journal of Advanced Research in Physical Science (IJARPS)*
*Volume 2, Issue 8, August 2015, PP 11-20*
*ISSN 2349-7874 (Print) & ISSN 2349-7882 (Online)*
*www.arcjournals.org*

# A New Method to Extract the Electrical Parameters from Dark *I-V*:*T* Experimental Data of Cds/Cu(In,Ga)$Se_2$ Interface

**Ahmed A. El Tayyan**

Department of Physics, Al-Azhar University, Gaza, Gaza Strip, Palestinian authority
*ahmedtayyan@yahoo.com*

**Abstract***: This article suggests a simple method to calculate the electrical parameters of the single-diode model for ZnO\CdS\Cu(In,Ga)$Se_2$ solar cell from the I-V:T data in dark. These parameters are the ideality factor n, the saturation current $I_0$, the series resistance $R_s$ and the shunt resistance $R_{sh}$. This method relies on incorporating an empirical model into the single-diode model in order to remove its implicit nature and to ease calculations. To further justify the method, the forward I–V characteristics have been analyzed on the basis of standard thermionic emission (TE) theory. The extracted values of n at different temperatures from dark I–V:T characteristics of a CdS/p-Cu(In,Ga)$Se_2$ solar cell reveal that the conduction is dominated by tunneling enhanced interface recombination mechanism. The tunneling energies $E_{00}$ are calculated from the fit at two regions (region I: 0.2V<V<0.6V and region II: 0.6V<V<0.86V) and found to be about 155.1 and 119.9 meV for region I and region II, respectively. The influence of the temperature on the local ideality factor n has been analyzed and found that the ideality factor decreases exponentially when the temperature increases. Also, activation energies $E_a$ of about 2.22 eV for region I and 1.92 eV for region II are obtained from the corrected Arrhenius plot.*

**Keywords:** Solar *cell, Ideality factor, Schottky contact, thermionic emission, tunneling.*

## 1. Introduction

For an ideal Schottky diode, the flow of current is solely due to thermionic emission TE mechanism and the ideality factor *n* should be equal to unity. However, due to various factors such as device temperature, density of interface states dopant concentration, device area, structural properties of interface etc., the dark current-voltage *I-V* characteristics of Schottky contact exhibit deviations from ideal case with temperature dependent ideality factor [1,2].

Studying the dark electrical *I-V* characteristics of solar cells allows one to determine the device parameters and, hence, to predict the performance of the solar cell. These parameters can provide essential insights into the performance parameters which determine the efficiency of the device. The dark *I–V* curve is fitted into a model and the parameters of the model are determined in order to extract the electrical properties of the solar cells. Generally, two established models were used in literature: the single-diode model, which describes the solar cell as a single diode with parasitic resistances, and the two-diode model, which takes into account the recombination centers in the junction of the solar cell.

Several methods for extracting parameters from the *I–V* characteristics using the single-diode model have been reported. Some of these methods rely on illuminated *I-V* data and the subsequently calculated conductance of the device [3-6]. Other methods are based on numerical analysis [7-8]. An explicit analytic expression for *I* or *V* can be obtained with the help of the Lambert W function [9-13]. Jain et al. [9] have used the Lambert W function to study the properties of solar cells. However, their study is validated only on simulated *I-V* characteristics instead of extracting the parameters from the experimental *I-V* data. Later, El Tayyan [10] has used the Lambert W function approach to calculate the electrical parameters. In this method, the electrical parameters were determined with the aid of 4 equations that can be solved simultaneously while increasing the value of the photocurrent in small increments. Ortiz-Conde et al. [11] proposed a method to extract the solar cell parameters from the *I-V* characteristics based on the Lambert W function. First, they calculated the Co-content (CC) function from the exact explicit analytical expressions, and then extracted the device parameters by curve fitting. Other methods rely on dark *I-V* data. Bayhan and Kavasoglu [14], and Bayhan [15] have presented analytical methods for extracting the ideality factor $n$ of a pn-junction device based on the Lambert W-function and the dark *I-V* data. Gholami et al. [16] have studied the electrical parameters extraction from the dark *I-V* characteristics of Schottky barrier diode at various temperatures. Macabebe et al. [17] have used iteration and approximation techniques to determine the device parameters of the solar cells from the dark *I-V* data.

In this article, a simple method based on incorporating an empirical model into the single-diode model in order to estimate its electrical parameters $n$, $I_0$, $R_s$ and $R_{sh}$ for a ZnO\CdS\Cu(In,Ga)$Se_2$ solar cell from the dark *I-V:T* data. The *I-V:T* data are extracted from ref. [15]. To further justify the parameters extraction method, the *I-V* characteristics have been analyzed on the basis of standard thermionic emission (*TE*) theory and the extracted values of $n$ at different temperatures reveal that the conduction is dominated by tunneling enhanced interface recombination mechanism. The tunneling energies $E_{00}$ are calculated at two regions (region I: 0.2V<V<0.6V and region II: 0.6V<V<0.86V) and found to be about 155.1 and 119.9 meV for region I and region II, respectively. Also, the corrected Arrhenius plot of the current density $J_0$ in regions I & II of the Cu(In,Ga)$Se_2$ solar cell reveals activation energies $E_a$ of about 2.22eV and 1.92eV for region I and region II, respectively,

## 2. THEORY

With the assumption that the current is solely due to thermionic emission for a Schottky diode, the forward current as a function of voltage can be expressed as [1]

$$I = I_0 exp\left(\frac{qV}{nkT}\right)\left[1 - exp\left(-\frac{qV}{kT}\right)\right] . \tag{1}$$

For $V > 3kT/q$ Eq. (1) can be approximates as

$$I = I_0\left[exp\left(\frac{qV}{nkT}\right)\right] , \tag{2}$$

where the ideality factor $n$ is introduced to describe the deviation of the experimental *I–V* data from the ideal thermionic emission diffusion, $q$ is the electronic charge $1.6\times10^{-19}$C, $k$ is the Boltzmann's constant $1.38\times10^{-23}$ J/K, $T$ is the temperature in Kelvin, and $I_0$ is the saturation current defined by

$$I_0 = A^{**}S\,T^2 exp\left(\frac{-q\phi_b}{kT}\right) , \tag{3}$$

$\phi_b$ is the zero-bias barrier height, $A^{**}$ is the effective Richardson constant, and $S$ is the area of the diode. $\phi_b$ can be obtained from Eq. (3) as

$$\phi_b = \frac{kT}{q}\,ln\left(\frac{S\,A^{**}\,T^2}{I_0}\right) . \tag{4}$$

The values of the ideality factor $n$ and the saturation current $I_0$ can be obtained from the linear portion of $ln(I)$ *vs* $V$ plot at various temperature. The zero-bias barrier height $\phi_b$ at each temperature can be determined from Eq.(4) or from the Arrhenius plot form obtained by modifying Eq.(3) to get:

$$ln\frac{I_0}{T^2} = ln(A^{**}S) - \left(\frac{-q\phi_b}{kT}\right) . \tag{5}$$

If the transport is dominated by any of the thermally activated mechanisms such as interface, injection or space charge recombination, the ideality factor $n$ is independent of temperature with values ranging between 1 and 2 depending on the current transport and the dopant concentrations of the n and p-type layers [18]. For example, when the forward current is limited by thermionic emission $n$ is equal to 1. Shockley–Read–Hall (SRH) model assumes that the recombination in the space charge region is taking place via a single trap level located near the middle of the gap of low doped side of the junction gives ideality factor $n$ □ 2, and for an exponential distribution of defect, the value of $n$ may have values ranging between 1 and 2. On the other hand, when current transport is dominated by interfacial recombination the value of $n$ lies between $2 > n > 1$, and is dependent on the ratio $n = 1 + \varepsilon_p N_A/\varepsilon_n N_D$ where $N_A$ and $N_D$ are the acceptor and the donor concentrations, and $\varepsilon_n$ and $\varepsilon_p$ are the dielectric constants of n and p-type materials, respectively.

If recombination at the interface of the pn-junction is enhanced by tunneling, then, $n$ is described by [19],

$$n = \frac{E_{00}}{kT} coth\left(\frac{E_{00}}{kT}\right) \tag{6}$$

*Where* $E_{00}$ is a characteristic tunneling energy that measures the amount of tunneling contribution to the recombination process. For tunneling enhanced bulk recombination case, the ideality factor $n$ is given by the following equation [20]

$$\frac{1}{n} = \frac{1}{2}\left(1 - \frac{{E_{00}}^2}{3(kT)^2} + \frac{T}{T^*}\right), \quad (7)$$

where $kT^*$ is the characteristic energy of the exponential distribution of recombination centers in the bulk of the material. If the contribution of tunneling is negligible then Eq. (7) becomes

$$\frac{1}{n} = \frac{1}{2}\left(1 + \frac{T}{T^*}\right). \quad (8)$$

For tunneling dominated transport [18], the slope of *ln I–V* graph is essentially temperature independent, and the ideality factor $n$ become strongly dependent on temperature and may have values $n(T) \gg 2$.

## 3. Modeling

In the single-diode model, a diode accounts for polarization phenomena, a series resistance and a parallel resistance to account for power losses. The dark forward current of a pn-junction device can be expressed as

$$I = \frac{V - IR_s}{R_{sh}} + I_0\left\{exp\left[\frac{(V - IR_s)}{V_t n}\right] - 1\right\}. \quad (9)$$

$I_o$ is the dark saturation current of the device, and $V_t = kT/q$ is the thermal voltage, $R_s$ and $R_{sh}$ are the cell series resistance and the cell shunt resistance, respectively.

Equation (9) that describes the single-diode model is an implicit function, i.e. have the form $I = f(V, I)$. Such implicit nature of the single-diode model makes the method for adjusting the model parameters more difficult.

Other models that can generate the *I-V* curves from the manufacturer's datasheet of a PV system have been proposed. One of these models is the model that can be expressed as [21]

$$I_{TA} = I_{sc} - C_1 exp\left(-\frac{V_{oc}}{C_2}\right)\left[exp\left(\frac{V}{C_2}\right) - 1\right] \quad , \quad (10)$$

where $I_{sc}$ and $V_{oc}$ are the short circuit current and the open circuit voltage, respectively. The coefficients $C_1$ and $C_2$ of the model can be obtained either graphically or analytically. In this work Eq. (10) is modified to account for the dark situation by having the form

$$I_{TA} = C_1 exp\left(-\frac{V_{max}}{C_2}\right)\left[exp\left(\frac{V}{C_2}\right) - 1\right]. \quad (11)$$

Where $V_{max}$ is the maximum voltage on the dark *I-V* data. Details of finding the coefficients $C_1$ and $C_2$ and generating the dark *I-V* characteristics of a pn-junction can be found elsewhere [22]. Figure 1 shows the good match between the experimental and the modeled dark *I-V* data using Eq. (11).

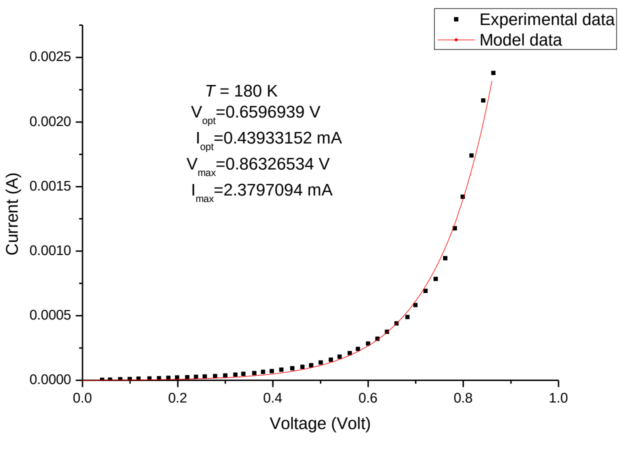


**Fig1.** *Experimental and model dark I-V characteristics of CdS/p-Cu(In,Ga)Se$_2$ solar cell at 180 K.*

To ease the calculations, the implicit nature of Eq. (9) could be removed by incorporating Eq. (11) into Eq. (9) to get

$$I = \frac{V - I_{TA}R_s}{R_{sh}} + I_0 \left\{ exp\left[\frac{(V - I_{TA}R_s)}{V_t n}\right] - 1 \right\}. \quad (12)$$

## 4. Adjusting the Method

In order to calculate the electrical parameters for a ZnO\CdS\Cu(In,Ga)$Se_2$ solar cell using the suggested method, one may proceed according to the following steps:

1- Figure 2, for example, shows the dark forward current density versus voltage characteristics of a typical ZnO/CdS/Cu(In,Ga)$Se_2$ heterojunction solar cell at 240 K. This figure reveals that for voltages greater than 0.2 V the dark forward current *I* can be expressed by Eq. (2). The conduction mechanism can be analyzed by dividing the *ln I* versus *V* curve into two distinct voltage regions 1: 0.2V < *V* < 0.6 V and 2: 0.6 V <V < 0.86 V. Thus *n* for each region could be calculated from the slope (*q*/*nkT*). On the other hand, $I_0$ could be calculated from the intercept at the ordinate. An important point should be mentioned here: the *I-V* data for both regions are extrapolated/ interpolated in equal steps between *V* = 0.2 volt and *V* = 0.86 volt. Thus, one can deal with each region separately in order to find the corresponding electrical parameters. At the end (see Figure 10) the data of both regions can be combined according to their voltage regions. Another point is that the value of *n* can be readjusted later due to the presence of $R_s$ and $R_{sh}$ in Eq. (9) and Eq. (12) (see step 3).

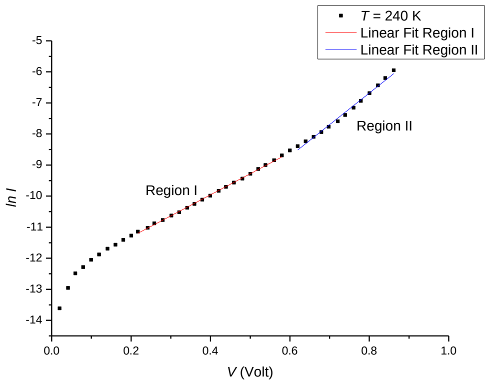


**Fig2.** *Dark ln I vs V of CdS/p-Cu(In,Ga)$Se_2$ solar cell at 240 K.*

2- A closer look at the *I-V* characteristics reveals that if one plot the areas *FF* defined by Eq. (13) (see Fig. 3)

$$FF = (I_{max} - I)V \quad (13)$$

at each point of the *I-V* plot one can find a point (at the knee of the curve) where this area is maximum. Here, $I_{max}$ is the maximum current of the *I-V* data. The variation of *FF* with voltage is shown in Fig. 4 (*FFe* corresponds to the areas obtained from the experimental *I-V* data). At this point one can easily determine the voltage and current at which this maximum area occurs.

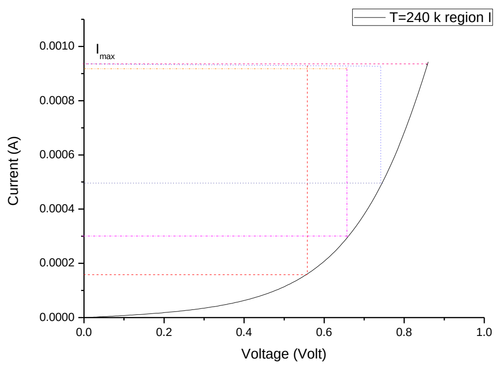


**Fig3.** *Here are some of the areas FF. The spaces between the upper lines are deliberately left in order to show the area.*

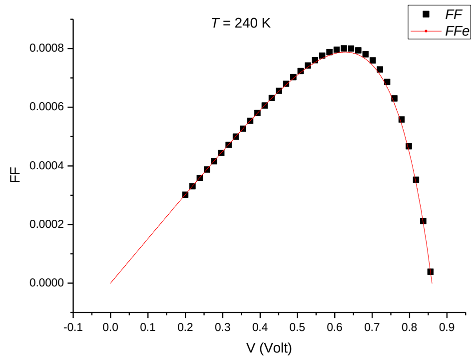


**Fig4.** *Variations of FF and FFe with voltage for CdS/p-Cu(In,Ga)$Se_2$ solar cell in region I at 240 K. Points are experimental values. Line is calculated data.*

3- Imposing the restriction that the experimental *FFe* is equal to the model *FF* at the maximum point one obtains

$$(I_{max} - I_e)V_e = (I_{max} - I)V \; . \tag{14}$$

Now, substituting Eq. (12) into this equation and solving for $R_{sh}$, one obtains the following equation:

$$R_{sh} = -\frac{V - ITA\,R_s}{I_0\left\{exp\left(\frac{V-ITA\,R_s}{V_t\,n}\right)-1\right\} - I_{max} + \frac{(I_{max}-I_e)V_e}{V}} \; . \tag{15}$$

By varying $R_s$ in steps one obtains values of $R_{sh}$. Figure 5 shows the variations of $R_{sh}$ vs $R_s$.

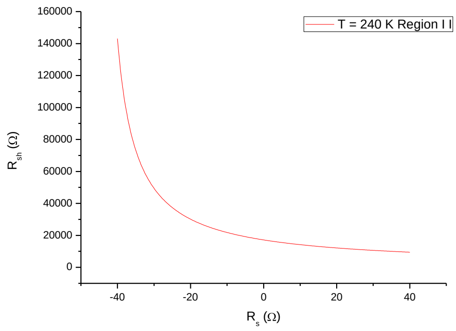


**Fig5.** *Variations of $R_{sh}$ with $R_s$ in region I at 240 K.*

When each pair of $R_s$ and $R_{sh}$ is substituted into Eq. (12) one obtains a family of *I-V* plots. These plots intersect at the same point. Figure 6 exhibits a plot of some of these *I-V* data. It is clear that these *I-V* plots intersect at the same point as seen from the inset.

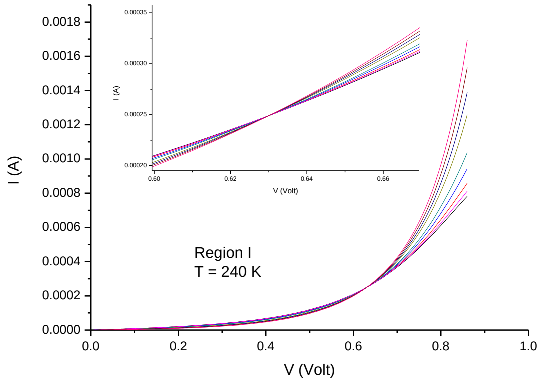


**Fig6.** *Various calculated I-V plots intersect at the same point. The inset shows that the plots intersect at the same point.*

Figure 7 shows some of the plots of *FF* and *FFe* versus voltage. Notice that the experimental *FFe* lies somewhere between the other plots. This means that there exists an *FF* plot corresponds to a certain pair of $R_s$ and $R_{sh}$ that falls exactly on *FFe* plot. Now, the goal is to find such pair.

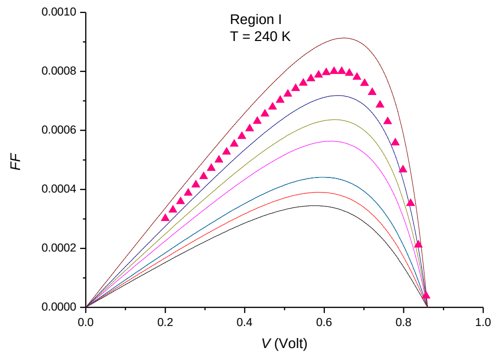


**Fig7.** *Modeled FF vs V and experimental FFe vs V. Each plot corresponds to a pair (*$R_s$*,* $R_{sh}$*). The points in data plot correspond to FFe.*

By inspecting Fig. 7, one can easily obtain the values of $R_s$ from the point of intersection of the plot of max *FF vs* $R_s$ and the plot of *FFe vs* $R_s$ as shown in Fig. 8. If the curves do not intersect, then one may need to readjust the value of *n* by slightly increasing it till intersection occurs. The shunt resistance $R_{sh}$ can be determined in a similar fashion as seen from Fig. 9.

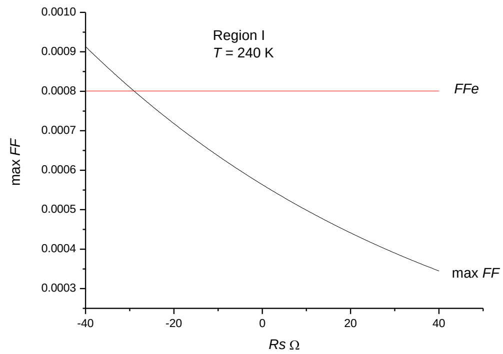


**Fig8.** *Variation of max FF vs* $R_s$ *and FFe vs* $R_s$*. The desired value of* $R_s$ *is determined from the point of intersection.*

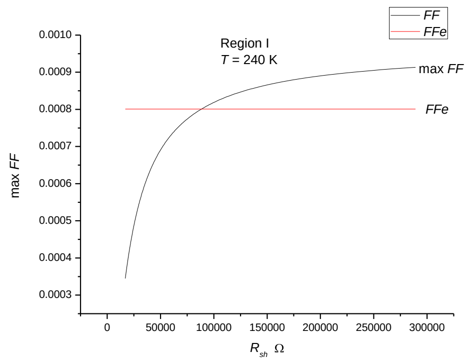


**Fig9.** *Variation of max FF vs* $R_{sh}$ *and FFe vs* $R_{sh}$*. The desired value of* $R_{sh}$ *is determined from the intersection point.*

**4-** In an attempt to verify the obtained values of the calculated electrical parameters and to express the robustness of the current method, simulations using Eq. (12) were performed. The calculated values of *n*, $I_0$ , $R_s$ and $R_{sh}$ used in the calculations are listed in Table 1 and the *I-V* characteristics are shown in Fig.10. At each temperature, the *I-V* data for region I and region II are recombined according to their voltage interval and plotted as a single *I-V* curve (see Fig. 10).

**Table1.** *Calculated dark parameters of ZnO\CdS\Cu(In,Ga)$Se_2$ solar cell at various temperatures.*

| Temp. K | Region | slope | Intercept | $I_0$ x $10^{-6}$ | *n* | $R_s$ | $R_{sh}$ x $10^4$ |
|---|---|---|---|---|---|---|---|
| 100 | I | 6.31143 | -13.02834 | 2.19717086 | 18.65 | 17 | 8.28686 |
| | II | 7.99843 | -14.05725 | 0.78526076 | 14.77 | -31.8 | 6.45983 |
| 140 | I | 6.3414 | -12.90482 | 2.48603869 | 13.08 | -52 | 9.62725 |
| | II | 8.12651 | -13.99046 | 0.83949946 | 10.41 | -25.6 | 4.26364 |
| 160 | I | 6.38351 | -12.82656 | 2.6884117 | 11.32 | -37.6 | 20.1154 |
| | II | 8.05468 | -13.84913 | 0.96693941 | 9.18 | -20.4 | 8.28892 |
| 180 | I | 6.46837 | -12.81069 | 2.7314171 | 9.82 | -58.4 | 29.062 |
| | II | 8.52083 | -14.07875 | 0.40414181 | 6.85 | 13.8 | 3.12294 |
| 200 | I | 6.33146 | -12.65725 | 3.1843894 | 9.16 | -0.2 | 8.79837 |
| | II | 8.82775 | -14.19624 | 0.68336275 | 6.66 | -16.6 | 4.66868 |
| 240 | I | 6.7846 | -12.67148 | 3.13939642 | 7.08 | -28.8 | 8.71373 |
| | II | 10.17271 | -14.81999 | 0.36623523 | 4.88 | -12.4 | 4.66868 |
| 260 | I | 7.39371 | -12.27516 | 4.66622577 | 6.17 | 2.6 | 1.040179 |
| | II | 10.24406 | -13.93542 | 0.88700076 | 4.49 | -2.6 | 0.61486 |
| 300 | I | 7.97819 | -12.007222 | 6.1000 | 4.884 | -7 | 1.22339 |
| | II | 9.15928 | -12.454534 | 3.90 | 4.3 | 0.4 | 4.39234 |

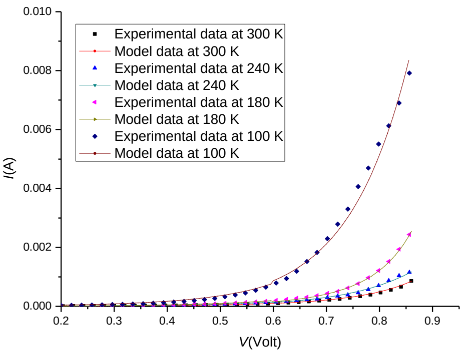


**Fig10.** *Experimental and model dark I-V plots of ZnO\CdS\Cu(In,Ga)$Se_2$ solar cell at various temperatures. Points are experimental data. Line is model data.*

## 5. Results and Discussions

In order to pursue further in justifying the extraction method, the ideality factor *n* that has been readjusted due to the presence of $R_s$ and $R_{sh}$ (see step 3 in sec. 4) is analyzed by considering its variation caused by tunneling current responsible for the thermionic field emission phenomena. The relation of the variation of *n* with respect to temperature is illustrated in Fig. 11 for region I and region II. The extracted *n*–*T* data is found to fit well on the theoretical curve generated using the relation given by Eq. (6). The tunneling energies $E_{00}$ are calculated at region I and region II and found to be about 155.10 and 119.99 meV, respectively. Bayhan and Kavasog˘lu [23] have suggested that the electrical conduction in CdS/p-Cu(In,Ga)$Se_2$ device to be dominated by tunneling enhanced interface recombination mechanism in dark.

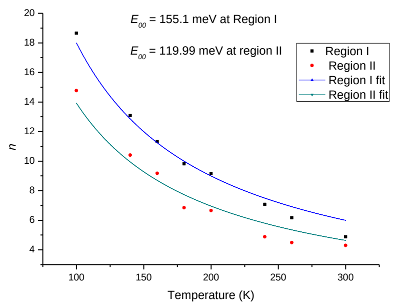


**Fig11.** *The variations of the ideality factor with temperature under dark for region I and region II. Points are the calculated values. Line is the fit.*

To further analyze the ideality factor $n$ expressing the robustness of the extraction method, one can follow the approach introduced by Rau et al. [20,24]. This approach explains the tunneling enhancement of recombination in the bulk via deep centers in the space charge region or at heterojunction interface. This approach assumes that the forward current of the heterojunction is also determined by Eq. (2). The activation energy $E_a$ can be determined from the calculated data by reorganizing Eq. (2) to have the following form

$$n\ln(J_0) = \frac{-E_a}{kT} + n\ln(J_{00}) \quad . \qquad (16)$$

Thus, $E_a$ can be deduced from the slope of a linear plot of $n\ ln(J_0)$ versus $1/T$. According to this approach, $E_a$ either represents the band gap energy of absorber material $E_g$ in case of bulk recombination or the interface barrier height $\Phi_b^p$ [24] for holes in case of interface recombination. Activation energies of about 2.22 eV and 1.92 eV were extracted for region I and region II, respectively, from the modified Arrhenius plots of $n\ ln(J_0)$ vs $1/T$ shown in Fig. 12. These values of activation energies are close to those obtained by Bayhan and Kavasog˘lu [23]. The value of the band gap energy of $Cu(In,Ga)Se_2$ is different from $E_a$ in either region. Thus, it is more likely that $E_a$ represents the interface barrier height $\Phi_b^p$ and the recombination process is controlled by the heterojunction interface [23].

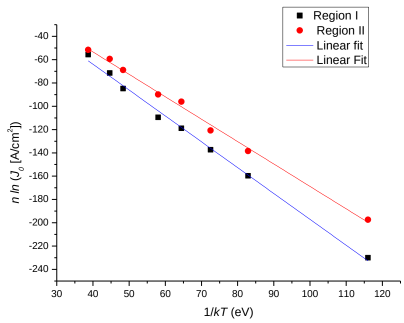


**Fig12**. *Corrected Arrhenius plot of the current density $J_0$ in region I & II of the Cu(In,Ga)Se2 solar cell.*

It is clear that the calculated values of $R_s$ (see Table 1) may have either positive or negative values. Physically $R_s$ of a solar cell can only have a finite positive value which for a given cell varies with the cell temperature and illumination intensity and is independent of the dark saturation current. Many authors have reported negative $R_s$ resistance at various temperatures [25-31]. Sharma et al. [25] have reported that the variation of $R_s$ with temperature is negative at low and medium temperatures for some solar cells. Phang et al. [26], also, reported that fitting the single diode model to cell characteristics collected at low illuminations can result in negative series resistance values**,** while even at higher illuminations up to one sun, the use of the single diode model can result in significantly different series resistance values [27]. Hamdy and Call [28] have reported that not only some of $R_s$ values are negative, but also the magnitudes are far from close to the exact value. Wagner [29] has suggested that as negative resistors do not exist in reality, the component in the equivalent circuit diagram cannot be an ohmic resistance. The equivalent circuit diagram has to be modified by a fictitious photoelectric component which presents either a positive or a negative resistance. As negative resistance is not physically possible, one might believe that the single diode model is particularly inaccurate in describing cell behavior at dark, or the $R_s$ component in the single-diode model cannot be an ohmic resistance in nature.

## 6. Conclusion

The electrical transport mechanisms of $ZnO\backslash CdS\backslash Cu(In,Ga)Se_2$ have been investigated in the temperature range 100-300 K and in dark. The electrical parameters of the single-diode model $n$, $I_0$, $R_s$ and $R_{sh}$ have been calculated by a new method. This method relies on incorporating an empirical model into the single-diode equation in order to remove its implicit nature and to make calculations easier. The dark *I–V* characteristics have been analyzed on the basis of standard thermionic emission (*TE*) theory. The extracted $n$ values at various temperatures reveal that the conduction is dominated by tunneling enhanced interface recombination mechanism with tunneling energies $E_{00}$ of about 155.1 and 119.9 meV for region I and region II, respectively. Also, activation energies $E_a$ of about 2.22eV for region I and 1.92eV for region II are obtained from the corrected Arrhenius plot.

## REFERENCES

[1]. E. H. Rhoderick and R. H. Williams, Metal Semiconductor Contacts, second ed., Clarendon Press, Oxford, 1988, Ch. 3.

[2]. Aniltur O.S. and Turan R., Electrical transport at a non-ideal CrSi2-Si junction, Solid State Electron 44(1) 41 (2000).

[3]. Chan D. S. H. and Phang J. C. H., Analytical methods for the extraction of Solar-Cell Single- and Double-Diode Model Parameters, IEEE Transactions on Electron Devices Ed-34, Pp 286-293 (1987).

[4]. Chegaar M., Ouennoughi Z. and Guechi F., Extracting dc parameters of solar cells under illumination, Vacuum. 75(4), 367 (2004).

[5]. El Tayyan A. A., PV system behavior based on datasheet, Journal of Electron Devices. 9, 335 (2012).A. A. El Tayyan, A simple method to extract the parameters of the single-diode model of a PV system, Turkish Journal of Physic. 37, 121 (2013).

[6]. Singal C. M., Analytical expression for the series-resistance-dependent maximum power point and curve factor for solar cells, Solar Cells. 3 163 (1981).

[7]. Quanxi J. and Enke L., A method for the direct measurement of the solar cell junction ideality factor, Solar Cells. 22(1) 15 (1987).

[8]. Jain A. and Kapoor A., A new method to determine the diode ideality factor of real solar cell using Lambert W-function, Solar Energy Materials and Solar Cells. 85 391 (2005).

[9]. El Tayyan A. A., Parameters Extraction of Solar Cells from Their Illuminated *I-V* Curves Using the Lambert W Function, Turkish Journal of Physics. 39 1 (2015).

[10]. Ortiz-Conde A., S´anchez Garcia F. J. and Muci J., New method to extract the model parameters of solar cells from the explicit analytic solutions of their illuminated *I–V* characteristics, Solar Energy Materials and Solar Cell. 90(3) 352 (2006).

[11]. Aazou S. and Assaid E. M., Model physical parameters effects on real solar cell characteristics and power curve, Global Journal of Physical Chemistry. 2 61 (2011).

[12]. Ghani F., Duke M. and Carson J., Numerical calculation of series and shunt resistances and diode quality factor of a photovoltaic cell using the Lambert W-function, Solar Energy. 91 422 (2013).

[13]. Bayhan H. and Kavasoglu S., Exact Analytical Solution of the Diode Ideality Factor of a pn Junction Device Using Lambert W-function Model, Turk. J. Phys. 31 7 (2007).

[14]. Bayhan H., Study of CdS/Cu(In, Ga)$Se_2$ interface by using n values extracted analytically from experimental data, Solar Energy. 83 372 (2009).

[15]. Gholami S. and Khakbaz M., Measurement of I-V characteristics of a PtSi/p-Si Schottky Barrier diode at low temperature, International Scholarly and Scientific Research. 5, 9 (2011).

[16]. Macabebe E. Q. B. and van Dyk E. E., Parameter extraction from dark current–voltage characteristics of solar cells, South African Journal of Science. 104, 401 (2008).A.L. Fahrenbruch and R. H. Bube, Fundamentals of Solar Cells, third ed., Academic, New York,1983, ch. 5.

[17]. Padovani F. A., and Stratton R., Field and thermionic-field emission in Schottky barriers, Solid State Electron. 9, 695 (1966).

[18]. Rau U., Jasenek A., Schock H. W., Engelhard F. and Meyer Th., Electronic loss mechanisms in chalcopyrite based heterojunction solar cells, Thin Solid Films. 361–362, 298 (2000).

[19]. El-Tayyan A., An Empirical model for generating the IV Characteristics for a Photovoltaic System, J. Al-Aqsa Unv. 10 (S.E.), 214 (2006).

[20]. El Tayyan A. A., Estimation of the local ideality factor of CdS/Cu(In,Ga)Se2 Interface from experimental data, European International Journal of Science and Technology. 4 No. 5, 138 (2015).

[21]. Bayhan H and Kavasogˇlu. A. S., Tunnelling enhanced recombination in polycrystalline CdS/CdTe and CdS/Cu(In,Ga)$Se_2$ heterojunction solar cells, Solid-State Electron. 49 991 (2005).

[22]. Nadenau V., Rau U., Jasenek A., and Schock H. W., Electronic properties of CuGaSe 2 -based heterojunction solar cells, Part I. Transport analysis Journal of Applied Physics. 87, 584 (2000).

[23]. Sharma S. K., Kalpana B. S., Srinivasamurthy N., and Agrawal B. L., Overcoming the problems in determination of solar cell series resistance and diode factor, J. Phys. D: Appl. Phys. 23, 1256 (1990).

[24]. Chan D. S. H., Phang J. C. H., Phillips J. R. and Loong M. S., A comparison of extracted solar cell parameters from single and double lumped circuit models, Tech. Dig. 1st Tnt. Photovoltaic Science and Engineering Conf. (Kobe, Japan), Pp. 151-153 (1984).

[25]. Charles J. P., Mekkaoui-Alaoui I., Bordure G. and Mialhe P., A critical study of the effectiveness of the single and double exponential models for the I-V characterization of solar cells, Solid-State Electron. 28, 807 (1985).

[26]. Hamdy M. A. and Call R. L., The effect of the diode ideality factor on the experimental determination of the series resistance of solar cells, Solar Cells. 20, 119-(1987).

[27]. Wagner A., Peak-power and internal series resistance measurement under natural ambient conditions, EuroSun 2000 Copenhagen, June 19-22,Pp 1-7( 2000).

[28]. Bashahu M. and Arimana H., Review and test of methods for determination of solar cell series resistance, Renewable Energy. 6 N0. 2, 129 (1995).

[29]. Yamamoto Y. and Miyanaga H., An Analysis of Positive and Negative Resistance Characteristics in the High-Current-Density Region of Schottky Diodes. IEEE Transactions on electron devices 37. NO. 5., Pp.1364-1372 (1990).

## AUTHOR'S BIOGRAPHY

**Ahmed A. El Tayyan** received the B.S. degree in physics from Al Azhar University, Cairo, Egypt in 1982, the M.S. degree in physics from Oregon State University, Corvallis, Oregon, U.S.A in 1988 and the Ph.D. degree in Physics from University of Khartoum, Khartoum, Sudan in 1998. He is conducting research in the areas of Photovoltaics & Solar Cells, Conducting & Photoconducting Polymers and Ellipsometry.